Development of Wear Resistant Alloys for Use in Laser Powder Bed Fusion

Corina Junghetu[1] Corina.Junghetu@hoeganaes.com; Chris Schade[2] Chris.Schade@hoeganaes.com; Kerri Horvay[2] Kerri.Horvay@hoeganaes.com; Tom Murphy[2] Tom.Murphy@hoeganaes.com

[1] Hoeganaes Corporation Europe, Romania
[2] Hoeganaes Corporation, USA

Abstract

In general, hard materials for tooling and wear resistant applications are very difficult to machine, with the most common forming method being grinding. Utilizing a grinding operation severely limits the shape of the final product which can be achieved. Additive manufacturing (AM), specifically Laser Powder Bed Fusion (LPBF) allows for intricate shapes to be formed for most all alloy materials. However, due to their brittle nature many of the materials with high hardness tend to crack in the LPBF process. This paper highlights the mechanical properties and microstructures of a family of wear resistant alloys that can be used in LPBF for a range of applications (from alloy steels to stainless steel). In addition to mechanical properties, case studies of the materials in real life applications are presented and the wear mechanisms reviewed and compared to their machined counter parts.

Introduction

Wear of an alloy or metal is generally considered as the removal of material due to forces which act upon the material from another contacting surface or substance. The contacting substance may be another surface, hard particles, fluids and other media.[1] Wear is progressive removal of material from the friction of the contacting substance. In general, the wear resistance is correlated with the hardness. The harder the substance in contact with the piece under study, the greater the wear. In reality there are other factors such as operating temperature, environment, contact pressure and material microstructure. Therefore it is very difficult to predict the wear simply by looking at the hardness of the materials in question. Figure 1 shows some of the various wear mechanisms that can exist in metal systems.

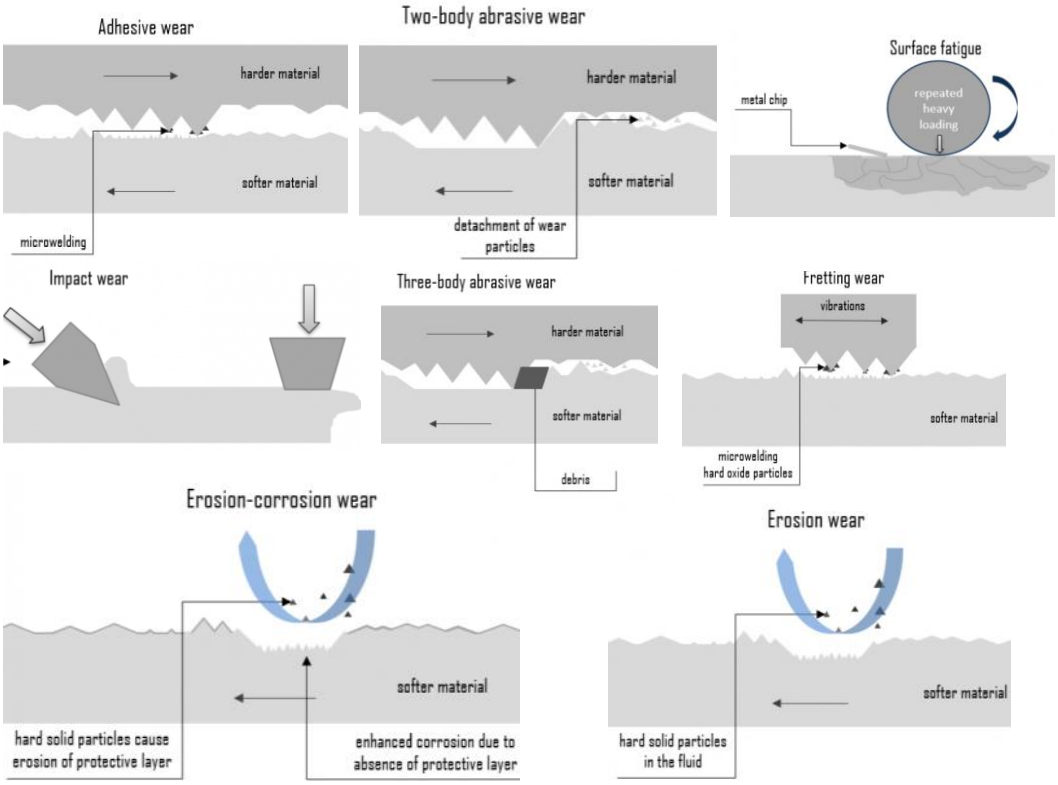

Figure 1: Potential Wear Mechanisms for Materials. [2].

Although mechanical properties of an alloy are not the complete descriptor of how they will perform under various wear conditions, they are a useful starting point for defining potential materials for a certain application. Hardness, mechanical strength and impact strength can help to assess the potential of the material. Specific wear testing that replicates the service conditions of the part are also useful for evaluating materials for specific applications and will be considered in future studies.

Additive Manufacturing of wear resistant materials is a valuable tool as small prototypes can be made without large costs. These prototypes can be placed in service to collect data on the performance of both the material and design of the part. This can be done without incurring large costs due to molds or machining of very hard materials. The design features of AM lend itself to creating parts that could not be produced simply by grinding the shape from a block of metal. Therefore, there is great potential in utilizing additive manufacturing for producing serial parts for industrial use.[3]

This study will document and introduce a new family of alloys called Ancorwear. These materials are designed specifically for LPBF and cover a range of hardness that mimics wrought alloys available for wear resistant applications. The mechanical properties of these alloys, as well as case studies and wear testing, are reviewed to show applicability of these materials to real world applications.

Experimental procedure

Several alloys were developed covering a range of hardness and ultimate tensile strength values. There are a number of factors to be considered when choosing an appropriate alloy for an application. These can include: the structural properties, operating temperature, atmosphere or corrosion resistance and toughness. The main starting point for these attributes is the chemical composition of the alloys as shown in Table 1, which presents the chemical compositions of the alloys examined in this study, to cover a wide range of applications. Ancorwear 500 and 600 are alloys made to mimic conventional wrought abrasion resistant grades commonly produced in plate steels. [4-5] These grades of steel are typically difficult to form and used in fairly simple shapes. Ancorwear SPL is a chromium/nickel free alloy similar to the 500 and 600 grades but is designed to meet health and safety requirements where chromium and nickel are not permitted. S7 is a typical tool steel but has the advantage of good impact and shock resistance.[6] S7 has good resistance to softening at moderately high temperatures with excellent combination of high strength and toughness. Ancorwear SS is a stainless steel that has high hardness but provides abrasion resistance when moderate corrosion resistance is also needed.[7]

Table 1: Overview of alloying compositions evaluated in this study.

Alloy	Fe	Mo	Ni	V	Mn	Cr	Si	C	0xygen
Ancorwear 500	Remainder	0.61	0.70	-	1.39	0.66	0.50	0.17	0.02
Ancorwear 600	Remainder	0.37	4.14	-	0.60	1.31	0.21	0.44	0.03
Ancorwear SPL	Remainder	1.48	0.09	0.14	1.01	0.08	1.23	0.23	0.03
Ancorwear S7	Remainder	1.57	-	0.30	0.78	3.15	0.69	0.51	0.03
Ancowear SS	Remainder	0.22	1.05	-	0.14	11.85	0.88	0.02	0.25

Powder Characterization

All powders used in this study were produced by gas atomization except for the Ancorweaar SS which was produced by water atomizing. Previous expereince with water atomized stainless steels showed that it was a viable method for LBPF. All powders were screened to a nominal 15-53 µm particle size, which is common for LPBF processing. Light optical microscopy (LOM) images of prepared cross-sections, the etched conditions, were acquired using a Leica MEF4M metallograph. Both glyceregia and Vilella's reagent were used for etching the cross-sections where required. Carbon levels were measured by combustion infrared analysis on a LECO CS 800. Chemical analysis was performed using Inductively Coupled Plasma-Optical Emission Spectroscopy (ICP-OES). Oxygen analsyis was performed by infrared analysis on a LECO ONH 836.

LPBF Processing

An EOS M290 AM machine with a building volume of 250 x 250 x 325 mm was used to make the specimens for this study by melting powder layer by layer with an Yb fiber laser (400W) within an argon filled chamber
Cubes samples (10 x 10 x 10 mm) were printed with a variety of different settings to evaluate the porosity content produced for all the alloys listed in Table 1. A constant layer thickness was used for all

the samples while the laser power, hatch distance and scanning speed were changed. Image analysis was used to measure the porosity content of the cross-section of the cubes perpendicular to the build direction. Settings for printing mechanical test specimens were chosen for all the alloys that led to a density of greater than 99.0%.

Mechanical Testing

A set of standard settings was used to build the tensile test specimens (MPIF Standard 10 flat dogbones).[8] Samples were cut from the build plate in the as-built condition after production. Tensile specimens were tempered for 1 hr at 538 ^{o}C in a nitrogen atmosphere prior to testing on all the grades except the Ancorwear SS. This material is first heated to 1260 ^{o}C for 30 mins in nitrogen atmosphere and furnace cooled to room temperature. This heat treatment forms a dual phase microstructure of martensite and ferrite. Following the initial heat treatment at 1260 ^{o}C, the Ancorwear SS was tempered at 538 ^{o}C for 1 hr in nitrogen to temper the martensite that was formed during the first step in the heat treatment.

Results

Mechanical Properties

To determine the maximum hardness achievable in each alloy tempering studies were performed on all materials. Due to the high level of residual stresses from the LPBF process and the nature of the alloys (high hardness) it is recommended that these materials not be used in the as printed state. Tempering was performed at temperatures ranging from 300 ^{o}C to 760 ^{o}C were for 1 hour in a nitrogen atmosphere. For each alloy, the tempering temperature which achieved maximum hardness is shown in Table 2. As expected, the S7 tool steel material has the highest hardness and lowest ductility. The Ancorwear 500, which is a hardenable low alloy steel, but with a carbon content which lends itself to welding has the lowest hardness but highest elongation, indicating a good toughness. The Ancorwear 600, which is more highly alloyed (Nickel), including a higher level of carbon, has hardness close to the S7 but with a much higher level of ductility as indicted by the elongation. The SPL, which has no nickel or chromium and a low level of carbon, has both high hardness and good ductility. The Ancorwear SS, which has low carbon (typical of stainless steels) has a HRC of 38, which is very high for a non-carbon stainless steel. The low carbon allows for a better corrosion resistance of this alloy compared to the other materials.

Table 2: Mechanical Properties of LPBF samples in the tempered condition.

Alloy	Tempering Temp. ^{o}C	UTS (MPa)	YS (MPa)	Elongation (%)	HRC
Ancorwear 500	538	993	903	18.1	21
Ancorwear 600	538	1469	1255	12.5	49
Ancorwear SPL	538	1482	1269	13.1	45
Ancorwear S7	538	1269	876	2.8	52
Ancowear SS	538	896	662	8.7	38

Microstructures

The microstructures of four samples listed in Table 2, alloys 500, 600, SPL, and S7, are tempered martensite with varying concentrations of fine precipitated carbides in ferrite. The chemical compositions of each alloy, as shown in Table 1, control the size, composition, and concentration of the carbides, with the higher carbon contents resulting in a higher carbide population density compared with the lower carbon contents. In addition, the ferritic regions are larger and more distinct in the lower carbon samples.

The fifth alloy, Ancorwear SS, has a dual phase stainless steel composition. Mechanical and physical properties of this alloy type are developed by heating the as-built sample in the two-phase region of the phase diagram, ferrite, and austenite, then cooling to transform the austenite to martensite. The image included in Figure 2 was heated to the temperature described in Experimental Procedure section and furnace cooled to produce the martensite/ferrite microstructure. The tannish regions are

lath martensitic and the featureless, white areas are ferrite. The alloy was then tempered at 538 °C before mechanical testing.

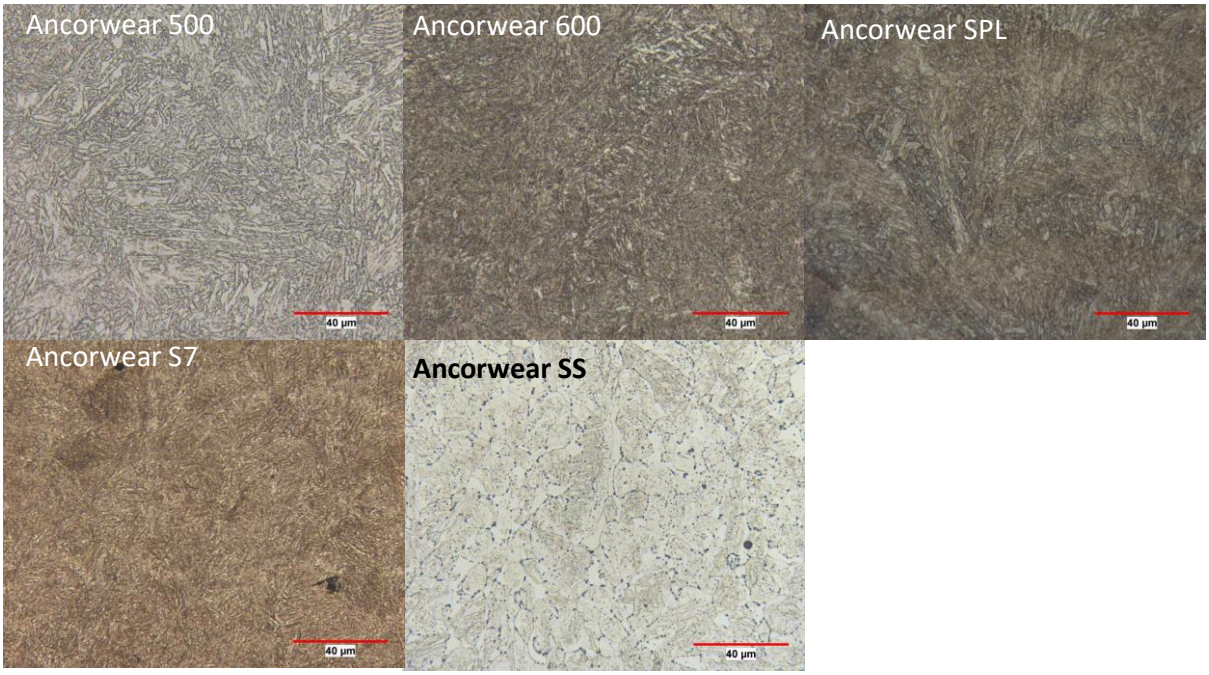

Figure 2: Microstructures of alloys whose properties are in Table II.

Case Study

Although unproven, AM techniques for making wear resistant parts should have a distinct advantage over current machining processes. Because the materials necessary for good wear resistance are generally of high hardness the machining of parts, other than very simple shapes, is very difficult. In many cases the only viable method for shaping the part is grinding which generally limits the design capability of the part and also leads to poor material yield. AM, particularly LBPF, would then seem to have an advantage in this regard as the design freedom can be increased with very low material waste. The alloys used in LBPF must be designed properly in order to prevent cracking during the laser melting and cooling process. Alloys with high carbon (> 0.60%) are generally to be avoided due to the fact that the fast-cooling leads to high thermal stresses which than can lead to crack formation upon cooling.

The alloys chosen in Table 1 show a range of hardness that can be used in a variety of applications. However, it is unclear how the AM production method will influence performance of part in service. Therefore, a case study in which several parts were made and placed in service. Figure 3 shows a

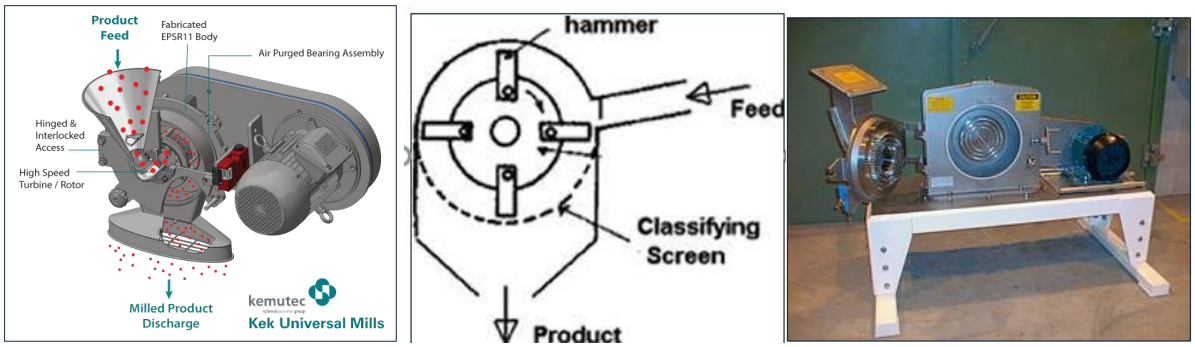

Figure 3: Example of a hammer mill.

typical mill for grinding material. Material is fed into the mill while hammers are rotating at high revolutions per minute (RPM). The material is shattered and forced through a mesh screen with different hole sizes corresponding to the final particle size targeted. The material then exists the mill

and is collected in a container. These types of mills are used to grind a variety of products including ferro-alloys for the steel industry. Therefore, the lifetime of the hammers and mesh screens utilized in the mill is critical. Typically, the hammers are ground or shaped from abrasion resistant plate steels and the screens, because the holes need to be perforated and then the screen needs to be formed (usually by rolling) are typically made from soft mild or stainless steels. In order to ascertain the use of LPBF, both the hammers and screens were printed from materials shown in Table 1 and grinding trials were performed and wear and lifetime of the AM printed parts were quantified. The material that was chosen to be ground was a metal alloy comprised of titanium-iron-manganese with a hardness of HV_{30} =355. Figure 4 shows the hammers in the rotating cage (left) and the perforated screens that the powder is forced through as it exits the mill (right).

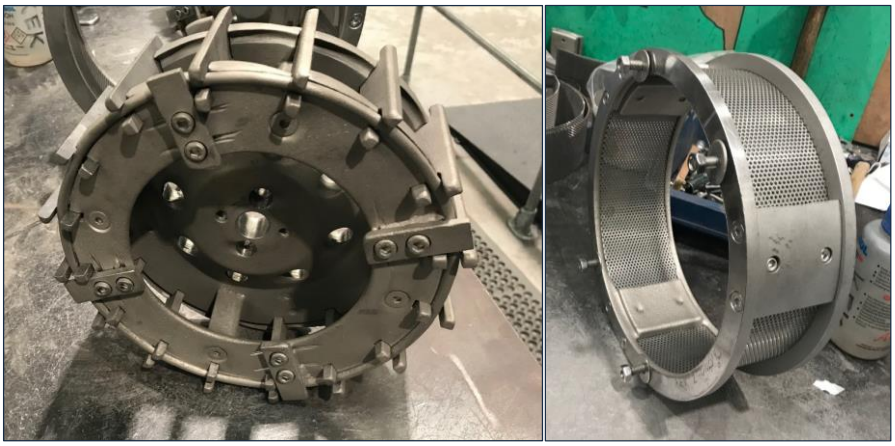

Figure 4: Rotating cage with hammers on the perimeter (left) and perforated screens (right).

For the field trials the Ancorwear SPL was chosen for this application due to its high hardness but good toughness (as indicted by its elongation values). Since the hammers are rotating at a high RPM, they need to have good impact toughness so that don't fail catastrophically. If a hammer were to shatter when operating at > 3000 RPM significant damage to the mill could occur. In addition to the hammers the perforated screens were also printed using LPBF. Typically, because the screens are formed by rolling, the material cannot have a high hardness as it makes forming difficult. However, since the LPBF can print the curved screen a higher strength/hardness material was thought as a potential improvement. Both sets of parts were printed on the EOS M290. In order to have a direct comparison of the standard hammers and screens, an equal number of hammers screens manufactured from both the standard process (machining and rolling) and LPBF were put in the hammer mill at equivalent positions. The wear and damage to each of the parts were monitored as a function of the amount of metal alloy that was ground.

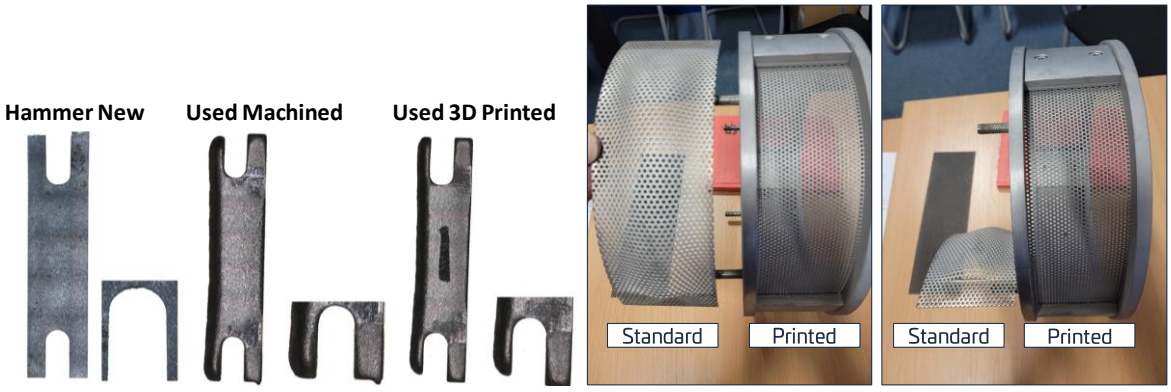

Figure 5: Hammers and screens.

Figure 5 shows photographs of the hammers and screens. In the case of the screens, the process was stopped after grinding 470 kgs of the metal alloy and the photograph on the left shows that the perforated hole diameter was much larger with the standard screen material when compared to the

SPL produced with LPBF. The right picture of the screens showed that standard processed screens failed at 1153 kgs of ground material while the laser printed screen was still serviceable. The rotating cage in Figure 4 holds 16 total hammers so the LPBF hammers were alternated with the standard hammers in the assembly (8 of each). All hammers lasted the lifetime of the campaign, and the weights were measured before and after the grinding campaign to get an indication of the weight loss. The wear on the standard material was 19.4% while the SPL alloy exhibited a weight loss of 25.0%. The differences in wear are not unexpected as the hardness of the standard material was 49 HRC versus a hardness of 46 HRC for the Ancorwear SPL. Since the performance of the LPBF SPL was unknown a conservative approach was taken to have a more ductile material (lower hardness) in order to avoid catastrophic failure on the initial trials. While the wear rate of the SPL was higher there were no catastrophic failures and there are further improvements in the heat treatments that can be undertaken to improve the hardness of the SPL.

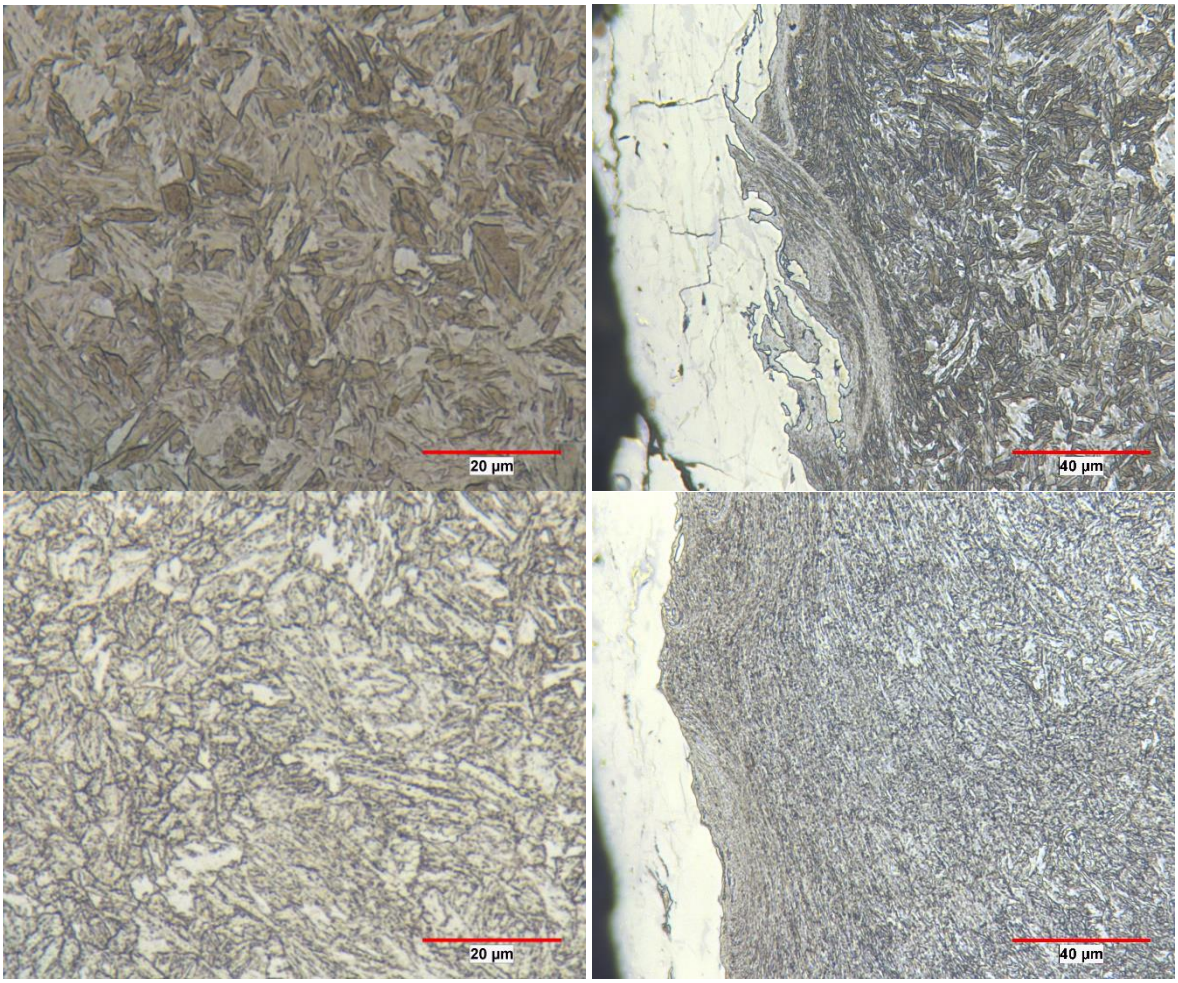

Figure 6: Microstructures of the two alloys in the core of the hammer (left) and at the wear surface of the hammer (right). (Top is Ancorwear 600 and Bottom is Ancorwear SPL)

A comparison of the two hammer microstructures is shown in Figure 6. The upper two images are taken from the standard machined alloy hammer and the lower two from the SPL alloy hammer. In each pair of images, the left is from the core, while the wear surface is depicted in the right image. The core microstructures (left images) are substantially different. In the standard alloy, details of the well-defined lath martensite are clearly visible and typical of a tempered low-carbon martensite. A representative area from the SPL alloy core shows evidence of a heavily tempered lath martensite, with large ferritic regions populated with a distribution of small carbides. This difference in microstructure accounts for the hardness disparity and was probably caused by the thermal history of the AM part. As stated earlier, the AM part was tempered at the conclusion of the build process at a temperature designed to attain the maximum hardness but still have ductility to resist the impact. However, the SPL microstructures in Figures 2 and 6 are clearly different, although both are accurate for the size part they represent. In building the hammer, as opposed to the substantially smaller tensile

bar, the temperature within the part remains elevated for a longer time due to the repetitive heating from the laser. Consequently, the part undergoes both a microstructural transformation during cooling from the melt and what may be considered a self-tempering as the part is continually reheated during the remainder of the build. Finally, at the conclusion of the build cycle, the hammer is tempered again at the predetermined temperature, which further tempers the already tempered microstructure.

In the two wear surface images (Figure 6, right), the white coating on the left side of each image is the built-up edge of the metal alloy powder on the hammer edge and the right side of each image is typical of the core, although at a lower magnification compared with the two core-only images. The microstructure differences are apparent, as is distortion to the microstructure in the form of flow of material from particle impact at the hammer edge during grinding. It is evident in these images that the flow and distortion in the AM hammer is at a greater depth compared with the machined hammer, which may help account for more material being eroded from the surface during use, thus contributing to a greater weight loss.

Based on the knowledge gained from the initial pilot trials and the finding that the AM materials already undergo a self-tempering from repetitive scanning of the laser over the prior built layer a more appropriate material selection for this application may be Ancorwear 600. Figure 7 shows the microstructure of the Ancorwear 600 in the as built condition and tempered at 315 ^{o}C for 1 hour. It is clear that the microstructure in both conditions is martensitic and more closely resembles the microstructure of the standard alloy. The Ancorwear 600 alloy has higher carbon then the other materials and therefore the hardenability of the alloy is greater and the hardness of the martensite that is formed is much greater when compared to the other alloys. The primary purpose of tempering is to impart toughness to the alloy. This occurs due to the relief of internal stresses caused by the formation of martensite and the precipitation and spherodization of carbides. Alloying elements have a direct effect on the latter. Elements such as manganese, nickel, and silicon have only a small effect since they do not form carbides. Elements such as chromium, molybdenum and vanadium are known to enhance hardness at higher tempering temperatures by forming alloy carbides. The effectiveness of these elements depends on their solubility in austenite and the nature of the carbide formed. These alloying elements also retard the coalescence of carbides, leading to temper resistance. [9] Nickel has a synergistic effect on the hardenability when added with chromium and molybdenum and is known to increase impact toughness for alloys with a martensitic microstructure. [10]

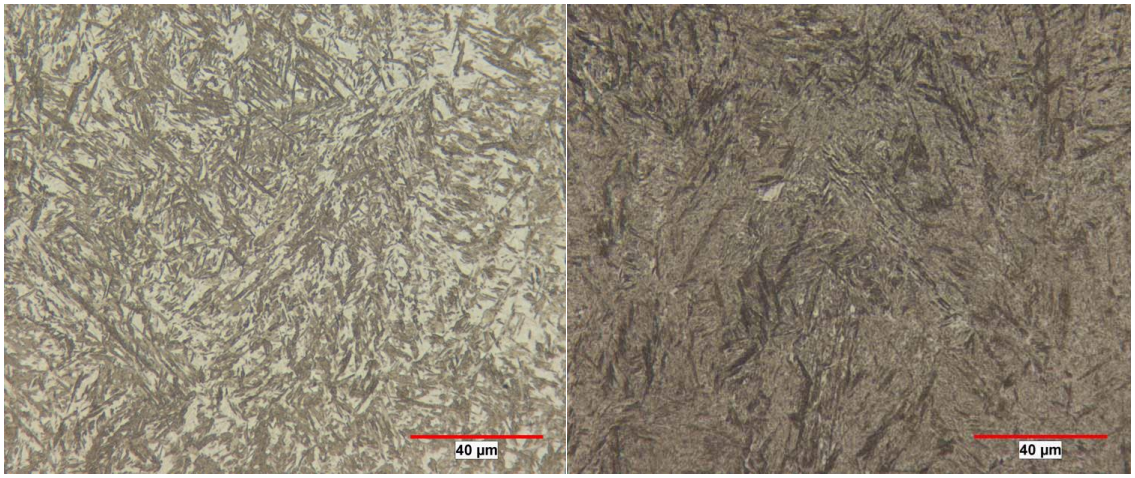

Figure 7: Microstructures Ancorwear 600 as built (left) and tempered at 315 ^{o}C (right).

In examining the physical properties of the Ancorwear 600 versus the Ancorwear SPL, the ductility of the two materials is similar, while the hardness of the 600 alloy is greater. This combined with the fact that the microstructure resists the tempering from the laser printing process, leads to a harder more wear resistant alloy that should also resist the impact seen in the performance of the grinding hammers.

Prior to running additional case studies with the Ancorwear 600, Charpy impact testing will be performed to ensure that the material will not fail catastrophically in the grinding machine. In addition,

wear tests, such as the pin and disk will be performed to correlate the wear rate test results and mechanisms (by metallography) with the actual operation of the hammers in the mill.

Conclusions

A family of wear resistant alloys for AM processing have been established. The selection of these materials to real world applications depends on a number of factors including hardness, chemical resistance, temperature of operation and environment. The free-form fabrication of the AM processes gives it a competitive advantage over machined components as it is difficult to grind these alloys to specific shapes without significant material losses. Further research is needed to correlate different wear mechanisms to the alloy selected and its hardness. Future work will include performing different wear testing on the various alloys to eliminate the need for costly trials and case studies prior to use.

References

[1] ASM Metals Handbook, Volume 18, Friction, Lubrication and Wear Technology, ASM Desktop Addition,2001, Edited by Peter J. Blau.
[2] https://material-properties.org/what-is-wear-resistant-materials-definition/
[3] W.E. Frazier, “Metal Additive Manufacturing: A Review”, Journal of Material Engineering, Performance, 2014 Vol. 23, No.6 pp.1917-1928.
[4] https://www.ssab.com/en/brands-and-products/hardox/product-program
[5] https://highstrengthplates.com/wp-content/uploads/2021/07/hardwear-brochure.pdf
[6] R. Carnes and G. Maddock, “Tool Steel Selection,” Advanced Materials and Processes, June 2004, pp.37-40.
[7] A. Lawley, E. Wagner, and C.T. Schade, “Development of a High-Strength-Dual-Phase P/M Stainless Steel,” *Advances in Powder Metallurgy and Particulate Materials – 2005*, compiled by C. Ruas and T. Tomlin, Metal Powder Industries Federation, Princeton, NJ, 2005, part 7 pp.78-89.
[8] *Standard Test Methods for Metal Powders and Powder Metallurgy Products,* 2016, Metal Powder Industries Federation, Princeton, NJ.
[9] R.A. Grange, C.R. Hribal and L.F. Porter, “Hardness of Tempered Martensite in Carbon and Low Alloy Steels,” Metallurgical Transactions A, 1977, vol. 8A, pp. 1775-1785.
[10] H.K.D.H. Bhadeshia and R.W.K. Honeycombe, Steels Microstructure and Properties, Elsevier Publishing, Third Edition, 2006.